Journal of Cellular and Molecular Medicine
A JOURNAL OF TRANSLATIONAL MEDICINE

J. Cell. Mol. Med. Vol 15, No 10, 2011 pp. 2095-2105

Mesothelial cell differentiation into osteoblast- and adipocyte-like cells

Lansley Sally M. [a], Searles Richelle G. [a], Hoi Aina [a], Thomas Carla [a, b], Moneta Helena [a, c], Herrick Sarah E. [d], Thompson Philip J. [a], Newman Mark [e], Sterrett Gregory F. [b, f], Prêle Cecilia M. [a, #], Mutsaers Steven E. [a, b, #, *]

[a] *Lung Institute of Western Australia and Centre for Asthma, Allergy and Respiratory Research, University of Western Australia, WA, Australia*
[b] *Anatomical Pathology Research, PathWest Laboratory Medicine, WA, Australia*
[c] *Division of Veterinary and Biomedical Sciences, Murdoch University, WA, Australia*
[d] *School of Medicine, Faculty of Medical and Human Sciences, The University of Manchester, Manchester, UK*
[e] *Department of Cardiothoracic Surgery, Sir Charles Gairdner Hospital, WA, Australia*
[f] *Department of Pathology, University of Western Australia, WA, Australia*

Received: October 8, 2010; Accepted: November 2, 2010

Abstract

Serosal pathologies including malignant mesothelioma (MM) can show features of osseous and/or cartilaginous differentiation although the mechanism for its formation is unknown. Mesothelial cells have the capacity to differentiate into cells with myofibroblast, smooth muscle and endothelial cell characteristics. Whether they can differentiate into other cell types is unclear. This study tests the hypothesis that mesothelial cells can differentiate into cell lineages of the embryonic mesoderm including osteoblasts and adipocytes. To examine this, a functional assay of bone formation and an adipogenic assay were performed *in vitro* with primary rat and human mesothelial cells maintained in osteogenic or adipogenic medium (AM) for 0–26 days. Mesothelial cells expressed increasing levels of alkaline phosphatase, an early marker of the osteoblast phenotype, and formed mineralized bone-like nodules. Mesothelial cells also accumulated lipid indicative of a mature adipocyte phenotype when cultured in AM. All cells expressed several key osteoblast and adipocyte markers, including osteoblast-specific runt-related transcription factor 2, and demonstrated changes in mRNA expression consistent with epithelial-to-mesenchymal transition. In conclusion, these studies confirm that mesothelial cells have the capacity to differentiate into osteoblast- and adipocyte-like cells, providing definitive evidence of their multipotential nature. These data strongly support mesothelial cell differentiation as the potential source of different tissue types in MM tumours and other serosal pathologies, and add support for the use of mesothelial cells in regenerative therapies.

Keywords: mesothelial cell • malignant mesothelioma • progenitor cell • osteoblast • bone • adipocyte • cell differentiation • epithelial-to-mesenchymal transition • tissue engineering

Introduction

The mesothelium consists of a monolayer of specialized cells known as mesothelial cells that line the peritoneal, pleural and pericardial cavities and most internal organs. Mesothelial cells are mesenchymal in origin but exhibit many characteristics of epithelial cells including a polygonal cell shape, expression of surface microvilli, epithelial cytokeratins and tight junctions [1]. Increasing evidence suggests that mesothelial cells are not terminally differentiated and have the capacity to differentiate into cells of different phenotypes, leading to the concept that a population of progenitor-like mesothelial cells exist [2]. During development, mesothelium lining the heart, liver and gut differentiate into endothelium and vascular smooth muscle through a process

[#] These authors contributed equally to this work.
*Correspondence to: Steven MUTSAERS, Associate Professor, Lung Institute of Western Australia, Ground Floor E Block, Sir Charles Gairdner Hospital, Nedlands, Perth 6009, WA, Australia.
Tel.: +61 (08) 9346 7948
Fax: +61 (08) 9346 4159
E-mail: mutsaers@liwa.uwa.edu.au

doi:10.1111/j.1582-4934.2010.01212.x

comparable to epithelial-to-mesenchymal transition (EMT) [3–5]. Transforming growth factor β_1 (TGF-β_1) stimulates adult mesothelial cells to adopt a myofibroblast phenotype *in vitro* [6] and explants of adult rat epicardial and mouse peritoneal mesothelium retain the ability to produce mesenchyme, including smooth muscle cells, in response to growth factors such as TGF-β_1 and platelet-derived growth factor [7, 8]. Recently it was demonstrated that transfection of the peritoneum and pleura of rats with an adenovirus expressing TGF-β_1 induced mesothelial cells to undergo EMT with subsequent fibrotic changes [9, 10]. EMT was also shown in peritoneal mesothelial cells obtained from the dialysis fluid effluent of patients undergoing continuous ambulatory peritoneal dialysis [11].

Some serosal pathologies are reported to contain areas of mesenchymal differentiation including cases of pleural malignant mesothelioma (MM) with osseous and cartilaginous differentiation [12–14]. It is thought that variability in the histological subtypes of MM and indeed the mesenchymal elements (osseous and cartilaginous) may reflect the multipotential nature of the mesothelium and the ability of mesothelial cells to differentiate into cell lineages of the embryonic mesoderm from which they are derived [15]. Donna and Betta [15] introduced the term 'mesodermoma' to classify primary tumours of the serous surfaces by considering the embryological development of serous membranes as being derived from the multipotent mesoderm. The source of cells and mechanism responsible for the osseous and cartilaginous differentiation in MM and the dystrophic calcification in the peritoneum of continuous ambulatory peritoneal dialysis patients is unknown. However, we suggest that under appropriate conditions, mesothelial cells are capable of differentiating into different cell types within the mesenchymal cell lineage including cells with osteoblast and adipocyte-like phenotypes. In the present study we confirm that some MM tumours contain mineralized bone and demonstrate the ability of both rat and human mesothelial cells to differentiate into osteoblast and adipocyte-like cells. Thus, mesothelial cells may be directly responsible for the different tissue types observed in pathologies such as pleural MM. Our findings confirm the multipotent nature of mesothelial cells and support the possibility of using the serosal mesothelium in regenerative therapies.

Materials and methods

Antibodies

Antibodies directed against human mesothelial cell clone Hector Battifora Mesothelial Epitope-1 (HBME-1), vimentin, pan-cytokeratin (DakoCytomation, Carpinteria, CA, USA), rat CD45, CD31, CD73 (BD Pharmingen, Franklin Lakes, NJ, USA), rat c-kit, mouse runt-related transcription factor 2 (RUNX2; Santa Cruz Biotechnology, Santa Cruz, CA, USA), human Stromal Cell Precursor Surface Antigen (STRO-1) (R&D Systems, Minneapolis, MN, USA), human α tubulin (Sigma-Aldrich, NSW, Australia), rat secreted protein, acidic, cysteine-rich (SPARC), CD49e fluorescein isothiocyanate (FITC), CD146 (Abcam, Cambridge, UK), rat secreted phosphoprotein 1 (SPP1), rat CD90 (Chemicon, Billerica, MA, USA) and rat integrin-binding sialoprotein (BSP; Developmental Studies Hybridoma Bank, University of Iowa, IA, USA) were used to characterize mesothelial cells and examine their osteogenic differentiation. Secondary and tertiary antibodies used were; biotin conjugated donkey anti-chicken (Chemicon, Vic, Australia), goat anti-rabbit horseradish peroxidase (HRP) (Pierce Biotechnology, Rockford, IL, USA), goat anti-mouse FITC (Sigma-Aldrich), goat anti-mouse Phycoerythrin (PE) (BD Pharmingen), rabbit anti-mouse HRP, swine anti-rabbit FITC and strepavidin-HRP (DakoCytomation).

Characterization of bone in malignant mesothelioma tumours

Sections of a human pleural MM biopsy were stained with haematoxylin and eosin for histology or von Kossa to identify areas of mineralized bone [16], and reviewed independently by three pathologists.

Isolation of mesothelial cells, bone marrow-derived mesenchymal cell (BMMC) and adipocytes

Pericardial fluid was obtained from nine adult patients, median age 65 years (range 57–81 years), undergoing coronary artery bypass graft surgery and mesothelial cells collected by centrifugation. Rat mesothelial cells were isolated from the omentum and peritoneal fat pads of 6–8 week male Lewis rats as previously described [17]. Bone marrow cells from the rat femora were collected in serum-free DMEM and mesenchymal cells selected on the basis of adherence to tissue culture plastic. Non-adherent cells were removed after 7 days in culture. Rat adipocytes were isolated from the epididymal fat tissue of male Lewis rats, collagenase digested, filtered and maintained in ceiling culture until required [18]. Approvals for human and animal studies were obtained from the Sir Charles Gardiner Hospital and University of Western Australia ethics committees, respectively.

Cell culture

Cells were maintained in standard medium containing DMEM with high glucose (4.5 mg/l) supplemented with 15% foetal calf serum (FCS), 4 mM L-glutamine, 100,000 units/l penicillin and 50 mg/ml streptomycin (Invitrogen Life Technologies, Mulgrave, Victoria, Australia) and 0.4 μg/ml hydrocortisone (Sigma-Aldrich). The rat osteosarcoma (ROS 17/2.8) and human foetal osteoblast (hFOB 1.19) cell lines were used as positive controls for osteoblast-related gene expression. TGF-β_1-stimulated (1 ng/ml for 48 hrs) mesothelial cells were used as a positive control for snail homolog 1 (SNAI1) expression. Isolated rat adipocytes were used as a positive control for the mature rat adipocyte phenotype and total RNA obtained from human subcutaneous fat was used as a positive control for adipocyte-related gene expression. Rat and human primary mesothelial cell cultures were used up to passage 3.

Characterization of isolated mesothelial cells

Mesothelial cells were characterized using immunocytochemistry and flow cytometry. Cells were immunolabelled with antibodies against the

mesothelial cell markers; cytokeratin, vimentin and HBME-1, and stem cell markers; CD31, CD45, CD49e, CD73, CD90, CD146, STRO-1 and c-kit.

Immunocytochemistry

Cells were plated onto serum coated glass cover-slips, cultured until 80% confluent and fixed in 4% paraformaldehyde (pH 7.4). Following washing and an initial blocking step in 10% FCS/tris-buffered saline (TBS) for 30 min., cells were incubated with primary antibody at the optimal concentration for 1 hr at room temperature. Cover-slips were washed in TBS and incubated with a biotin-conjugated secondary antibody followed by Strepavidin-HRP each for 1 hr.

Flow cytometry

Resuspended mesothelial cells were incubated in primary antibody diluted in phosphate-buffered solution (PBS)/5% FCS on ice for 30 min., washed and incubated with either FITC- or PE-conjugated secondary antibody on ice for 30 min. Washed cells were resuspended in PBS/5% FCS and analysed on a FACScan analyser (Becton Dickinson, Franklin Lakes, NJ, USA). Cells were also characterized ultrastructurally by transmission electron microscopy (TEM) using standard techniques [19].

Positive selection of HBME-1 stained mesothelial cells

Cells were stained as previously described and washed in basic sorting buffer [1 mM ethylenediaminetetraacetic acid, 25 mM Hepes (pH 7.0) and 1% FCS in Ca^{2+}-/Mg^{2+}-free Hanks balanced salt solution (HBSS)]. Stained cells were resuspended to 3×10^6 cells/ml and sorted on the basis of HBME-1^+ using a fluorescence-activated cell sorting (FACS) Vantage Cell Sorter (BD Biosciences, North Ryde NSW, Australia).

Functional assay of bone nodule formation

Mesothelial cells and BMMC were maintained in either standard medium or osteogenic medium (OM; standard medium supplemented with 10 mM sodium β-glycerophosphate (βGP), 50 μg/ml ascorbic acid and 10^{-8} M dexamethasone) for 0–26 days. Cells were either stained histochemically for alkaline phosphatase expression [16] and von Kossa (mineralization) or total RNA and protein harvested. Alkaline phosphatase levels were quantified by the addition of 200 μl *p*-nitrophenyl phosphate (Sigma-Aldrich) to 30 μg protein lysates and the amount of product (para-nitrophenol) determined at $OD_{405\ nm}$.

Assay of adipogenic differentiation and lipid accumulation

Mesothelial cells were maintained in either standard medium or adipogenic medium (AM; standard medium supplemented with 10 μg/ml insulin, 100 μM indomethacin, 100 μM 3-isobutyl-1-methylxanthine and 1×10^{-6} M dexamethasone) for up to 18 days. Lipid formation was examined and quantified at different time-points using oil red O histological staining. Accumulated lipid was stained with oil red O and quantified by extraction of the dye using isopropyl alcohol and measuring absorbance at 510 nm as described previously [20].

Analysis of osteoblast and adipocyte phenotype markers and markers of EMT

RT PCR and real-time PCR

Cells were lysed in Trizol (Invitrogen Life Technologies) and total RNA isolated in accordance with the manufacturer's instructions and DNAse treated (Qiagen, VIC, Australia). cDNA was synthesized from 1 μg total RNA using superscript III reverse transcriptase and random hexamers primers (Invitrogen Life Technologies). The mRNA expression of osteoblast, adipocyte and EMT markers was determined using gene-specific primers (Table S1) under standard PCR conditions. For real-time PCR, Taqman probes (Applied Biosystems, Vic, Australia) were used to examine RUNX2 mRNA levels in treated rat and human mesothelial cells and rat BMMC. PCR reactions were performed on an Applied Biosystems 7300 real-time PCR (Applied Biosystems). RUNX2 mRNA levels were normalized to 18S ribosomal RNA.

Western blot analysis

Cells were lysed in 50 mM Tris (pH 7.5), 0.5 mM ethylene glycol tetraacetic acid (EGTA), 150 mM NaCl and 1% Triton X-100 in distilled H_2O, supplemented with protease and phosphatase inhibitor cocktails (Sigma-Aldrich). Approximately 30 μg of protein was resolved per lane of a 10% SDS-PAGE gel and protein immobilized on a PVDF membrane (Amersham, Buckingham Shire, UK). Membranes were blocked overnight at 4°C in 5% skim milk/TBS-T (TBS with 0.05 % Tween 20), washed, then incubated with primary antibody for 1 hr at room temperature. α-tubulin was used as a loading control. Membranes were washed in TBS-T and incubated with either HRP-conjugated anti-rabbit or anti-goat antibody for 1 hr at room temperature. Membranes were washed, developed using chemiluminescent peroxidase substrate (CPS-1-120, Sigma) and visualized on hyperfilm ECL (GE Healthcare, Little Chalfont, UK). Densitometric quantification of RUNX2 was performed on scanned ECL hyperfilms using Molecular Dynamics ImageQuant version 5.1 analysis software. Pixel density of RUNX2 was normalized to α-tubulin for each sample to correct for loading differences.

Statistics

Data are presented as mean ± S.E.M. Comparisons between time-points were performed using a one sample *t*-test or a one-way ANOVA using a Tukey's multiple comparison test as appropriate to determine significance. A *P*-value <0.05 was considered significant.

Results

Bone formation in human pleural malignant mesothelioma

Biopsy specimen from a patient diagnosed with pleural MM containing bone-like elements demonstrated multiple foci of osseous metaplasia within the tumour associated with areas of mineralized bone (Fig. 1).

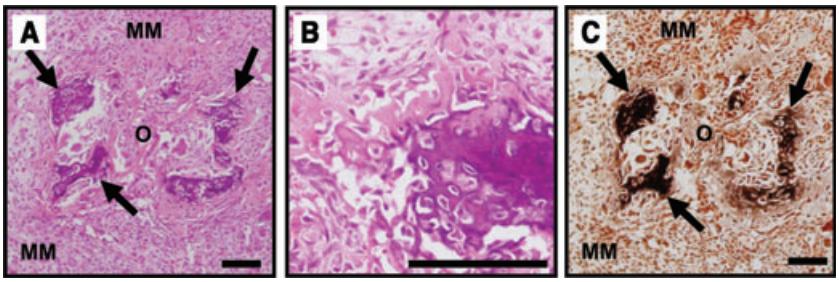

Fig. 1 Osseous differentiation in a human pleural MM biopsy with associated mineralization. (**A**) Haematoxylin and eosin staining of a biopsy from a patient with pleural MM demonstrating multiple foci of osseous metaplasia (O) within the tumour associated with areas of bone (arrow). (**B**) Higher magnification of osseous region showing osteoblastic/osteocytic cells within mineralized osteoid. (**C**) von Kossa staining demonstrating mineralized bone (black stain, arrow) within the tumour. Scale bar = 100 μm.

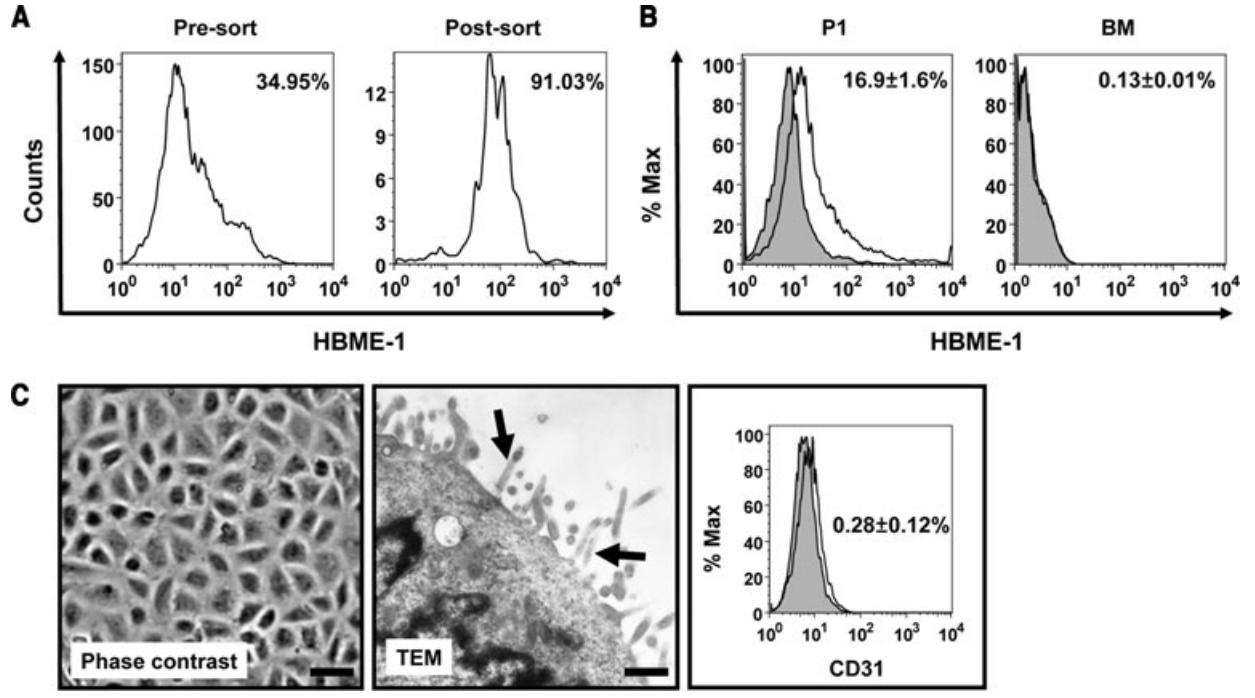

Fig. 2 Characterization of isolated rat mesothelial cells. (**A**) FACS histograms demonstrating the percentage of freshly isolated cells positive for HBME-1 surface marker expression pre- and post-FACS sorting for HBME-1. The resultant cell population was highly enriched for HBME-1 marker expression. (**B**) A representative FACS histogram showing a decrease in the percentage of HBME-1$^+$ cells following one passage in culture (P1; shaded = isotype control and unshaded = HBME-1$^+$). Freshly isolated rat BM cells do not express HBME-1 (expression shown as average% of expressing cells ± S.E.M.). (**C**) Phase contrast of cultured rat mesothelial cells showing a typical cobblestone morphology. Scale bar = 30 μm. Transmission electron micrograph of cultured mesothelial cells demonstrating characteristic surface microvilli (arrows). Scale bar = 1.5 μm. A representative FACS histogram of endothelial cell surface marker CD31 expression (unshaded) and isotype control (shaded) in freshly isolated mesothelial cells (expression shown as average % of expressing cells ± S.E.M.).

Bone nodule formation and mineralization by rat mesothelial cells using a functional *in vitro* assay

We have previously shown that mesothelial cells *in situ* express the marker HBME-1 [17]. Freshly isolated mesothelial cells were sorted based on surface expression of the mesothelial cell marker HBME-1 (Fig. 2A). A third of pre-sorted cells expressed HBME-1. HBME-1$^+$ cells were enriched to 91% after sorting for characterization studies and to over 96% for cell differentiation studies. Following culture, only 17% of the original HBME-1$^+$ cells retained HMBE-1 expression demonstrating down-regulation of this marker after culture (Fig. 2B). Total and HBME-1$^+$ cultured cells displayed a cobblestone-like morphology, expressed surface microvilli, junctional complexes and abundant intermediate filaments but did not express the endothelial cell marker CD31, all characteristic of mesothelial cells (Fig. 2C). Furthermore, the cells were immunopositive for cytokeratin and vimentin (data not shown).

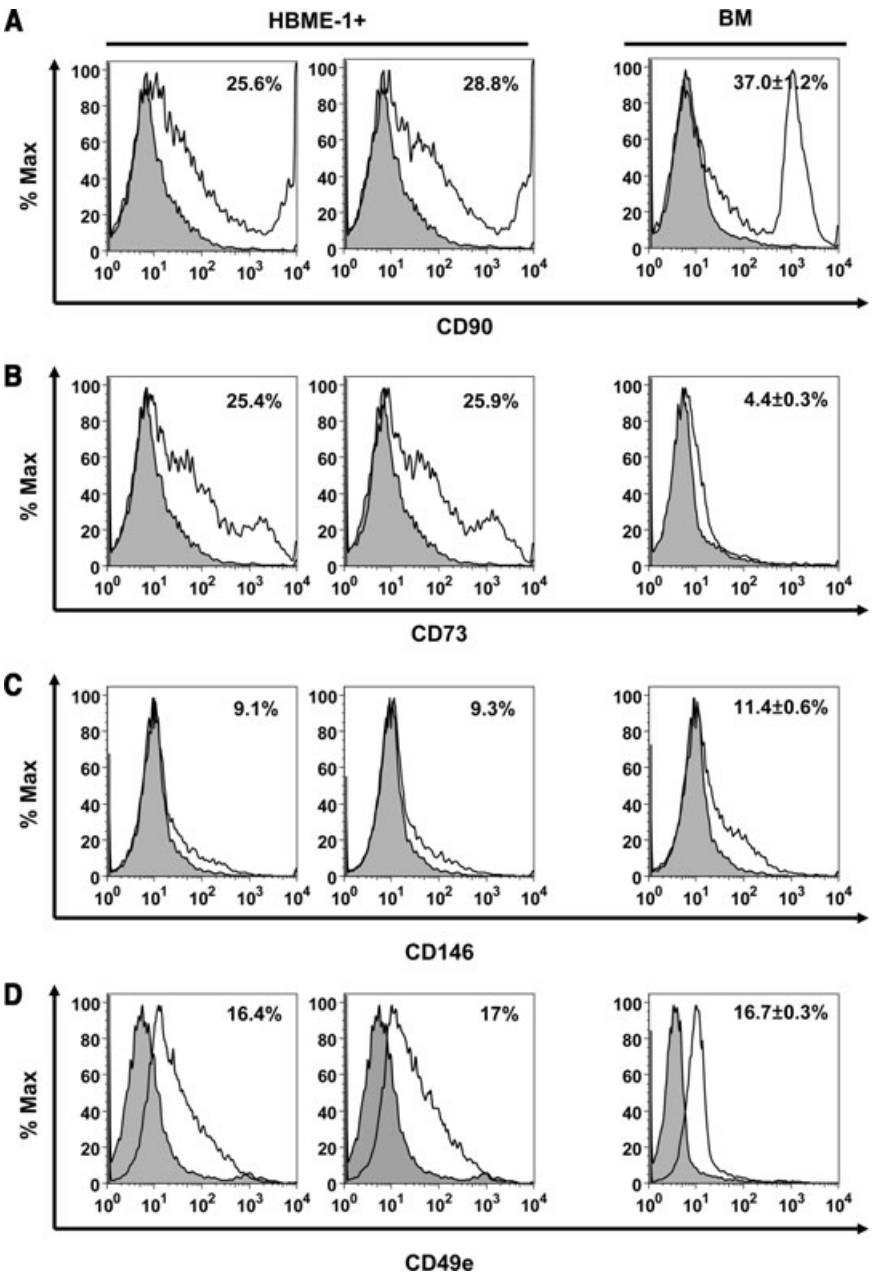

Fig. 3 Flow cytometry analysis of mesenchymal stem cell marker expression by HBME-1$^+$ mesothelial cells. FACS histograms demonstrating the percentage of HBME-1$^+$ (Passage 1) and BM cells expressing (**A**) CD90, (**B**) CD73, (**C**) CD146 and (**D**) CD49e (unshaded) and their respective isotype controls (shaded).

A proportion of HBME-1$^+$ mesothelial cells also demonstrated expression of the stem cell markers CD90, CD73, CD146 and CD49e (Fig. 3) but cultured cells were negative for c-kit and STRO-1 (data not shown). Cells were also negative for CD45, consistent with a mesenchymal origin (data not shown).

Rat mesothelial cells cultured in OM began to lose their characteristic cobblestone morphology by day 6 and condensed into nodule-like structures. This coincided with increased alkaline phosphatase expression, particularly in areas of cell condensation (Fig. 4A). Although alkaline phosphatase is suggestive but not specific for osteoblast differentiation, by day 18, the nodule-like structures stained positive for von Kossa, demonstrating mineralization (Fig. 4B).

This finding was consistent in both total and HBME-1$^+$ sorted cells (Fig. 4B). The time course of cell condensation, alkaline phosphatase expression and mineralized nodule formation was consistent with that of the rat BMMC control. Mesothelial cells cultured in standard culture medium did not show any change in morphology, condensation, alkaline phosphatase expression or nodule formation (data not shown).

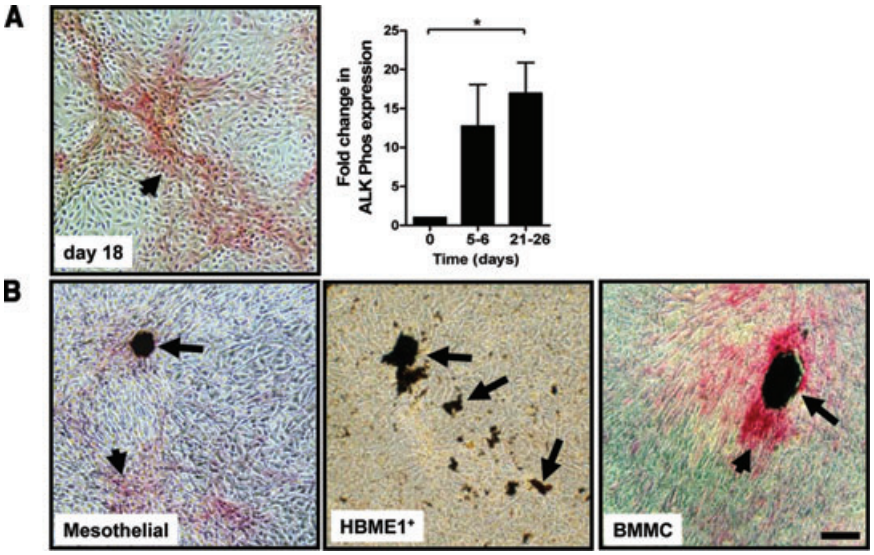

Fig. 4 Rat mesothelial cells express alkaline phosphatase and form mineralized nodules when incubated with OM. (**A**) Rat mesothelial cells cultured in OM for 18 days have lost their cobblestone appearance and express alkaline phosphatase (arrowhead, pink staining). Quantification of alkaline phosphatase expression in mesothelial cells cultured in OM demonstrates a significant increase over time, $*P < 0.05$. (**B**) Mineralized nodules (arrows, black staining by von Kossa method) form in regions of unsorted and HBME-1$^+$ mesothelial cells and BMMC after 18 days cultured in OM. Alkaline phosphatase expression is shown (arrow heads). Scale bar = 100 μm. Results shown are representative of three independent experiments.

Rat mesothelial cells express osteoblast markers

Osteoblasts are characterized by their ability to express an array of protein markers. The timing and expression profile of osteoblast-specific isoform of RUNX2, previously called core binding factor α_1/osteoblast-specific factor 2 (Cbfa1/OSF2), SPARC also known as osteonectin, SPP1, previously called osteopontin and integrin-BSP also called bone sialoprotein, identifies how far these cells have progressed along the osteoblast lineage. Rat mesothelial cells expressed SPARC, SPP1 and BSP mRNA and protein at day 0, which remained at similar levels over the 26 days in OM, consistent with expression in OM-differentiated BMMC (Fig. 5A, C). However, BSP mRNA and protein was low in mesothelial cells throughout the study. In BMMC and mesothelial cells RUNX2 expression increased with time in culture (Fig. 5A). Despite an overall increase in RUNX2 mRNA over time, the protein appeared to decrease (Fig. 5C, D). It must be noted that the RUNX2 antibody is not limited to recognizing the osteoblast-specific RUNX2 isoform. HBME-1$^+$ FACS sorted and unsorted rat mesothelial cells showed the same mRNA expression profile for SPARC and SPP1 but HBME-1$^+$ cells increased BSP expression over time (Fig. 5A). Furthermore, in HBME-1$^+$ cells, RUNX2 mRNA levels showed a biphasic response, increasing by day 6 then decreasing by day 9 and increased again by day 15, with levels at 18–26 days much higher than at day 0 (Fig. 5A).

Epithelial to mesenchymal cell transition during differentiation of mesothelial cells into osteoblast-like cells

To determine if OM-differentiated rat mesothelial cells undergo EMT, mRNA levels of the epithelial and mesothelial markers, cytokeratin 19 (CK19), E-cadherin, N-cadherin, α-smooth muscle actin (αSMA), matrix metalloproteinase 28 (MMP28), s100A4 and SNAI1, were investigated by RT-PCR (Fig. 6). CK19, E- and N-cadherin mRNA were all detected at day 0 in unstimulated cells. CK19 expression was maintained up to day 18 in OM cultured cells but was down-regulated by day 26. E-cadherin expression was down-regulated by day 5 but was significantly up-regulated again by day 18. N-cadherin mRNA remained constant throughout the time course. In contrast, αSMA, s100A4, MMP28 and SNAI1 mRNA was absent or extremely low in untreated cells at day 0 but was present by day 5. The onset of αSMA, s100A4, MMP28 and SNAI1 mRNA expression in treated rat mesothelial cells coincided with the initial down-regulation of E-cadherin.

Human mesothelial cells differentiate into osteoblast-like cells *in vitro*

The capacity for human mesothelial cells to differentiate into osteoblast-like cells was also examined. Cells were collected from the pericardial fluid of patients undergoing cardiac surgery. Approximately 24% of the total cell population were mesothelial cells, as determined by HBME-1 immunostaining, with the remainder of the cells consisting of monocytes/macrophages, lymphocytes and neutrophils (Fig. 7A, B). Mesothelial cells were enriched by cell culture and the phenotype confirmed by cytokeratin and vimentin immunostaining and TEM (data not shown). Mesothelial cells cultured in OM for up to 23 days demonstrated a similar pattern of mRNA and protein expression of RUNX2, SPARC, SPP1 and BSP as rat mesothelial cells (Fig. 7C–F). However, BSP mRNA and protein were up-regulated over the 23 day incubation period. Changes in osteoblast-specific RUNX2 mRNA levels varied between patient samples with a trend towards a small increase

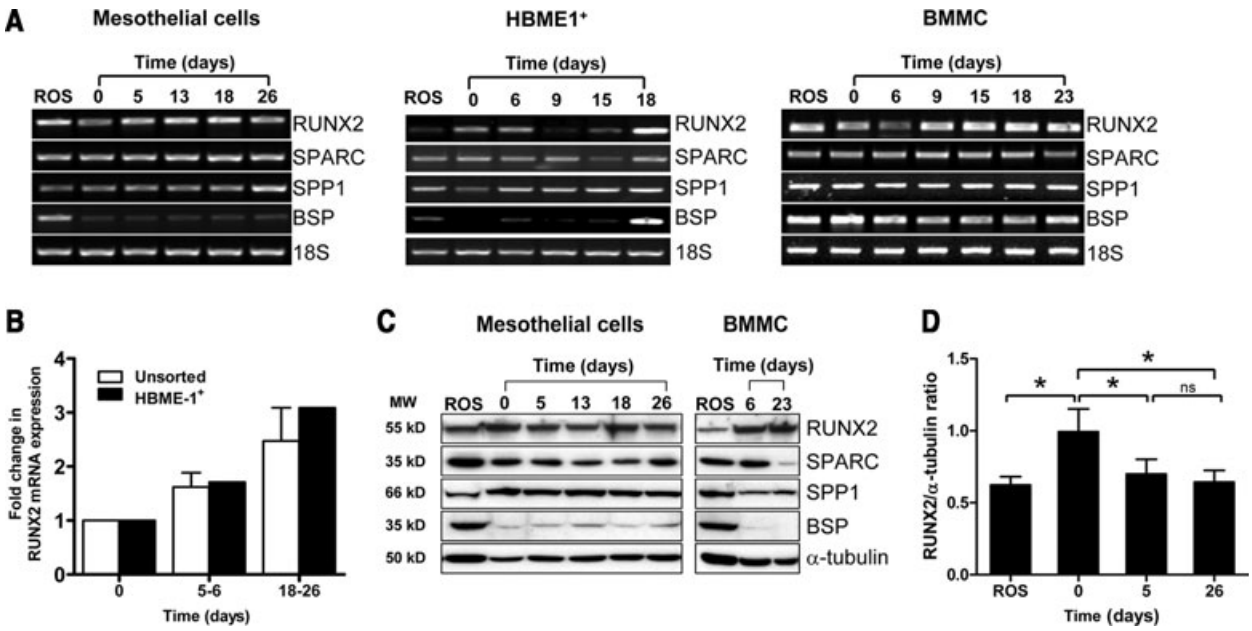

Fig. 5 Rat mesothelial cells express osteoblast markers. (**A**) RT-PCR analysis of unsorted and HBME-1$^+$ rat mesothelial cells and BMMC cultured in standard medium or OM showing expression of osteoblast-associated genes; RUNX2, SPARC, SPP1 and BSP. (**B**) Real-time PCR showing expression of RUNX2 mRNA in unsorted and HBME-1$^+$ rat mesothelial cells cultured in OM up to 26 days. (**C**) Western blot of osteoblast phenotype markers in rat mesothelial cells and BMMC cultured in standard medium and OM. (**D**) Quantitative analysis of RUNX2 protein in OM stimulated rat mesothelial cells up to 26 days in culture, $*P < 0.05$. 18S and α-tubulin were used as loading controls for RT-PCR and Western blot analysis, respectively. The rat osteosarcoma cell line ROS 17/2.8 (ROS) was used as a positive control for the mature osteoblast phenotype. Results are representative of at least three independent experiments.

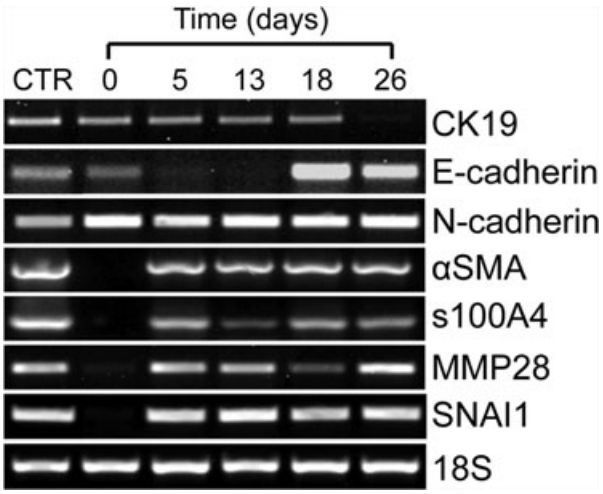

Fig. 6 mRNA expression of EMT markers during differentiation of rat mesothelial cells to osteoblast-like cells. mRNA expression of EMT markers CK19, E-cadherin, N-cadherin, αSMA, s100A4, MMP28 and SNAI1 by RT-PCR in mesothelial cells cultured for up to 26 days in standard medium or OM. Controls (CTR) include mesothelial cells grown in standard medium or treated with 1 ng/ml TGF-β_1 for αSMA, s100A4, MMP28 and SNAI1 expression. 18S was used as a loading control. Results are representative of at least three independent experiments.

over the incubation period (Fig. 7D). RUNX2 protein levels did not increase over time consistent with rat cells (Fig. 7F). Interestingly, alkaline phosphatase staining was absent in two of the three human mesothelial cell cultures at all time-points examined and von Kossa positive nodules were not detected in any of the samples (data not shown).

Rat and human mesothelial cells differentiate into adipocyte-like cells *in vitro*

Pre-adipocytes characteristically contain lipid which can be detected using the stain oil red O. Lipid accumulation was detected in AM cultured rat mesothelial cells as early as day 6 and increased significantly by day 18 (Fig. 8A). In contrast to the extensive oil red O staining detected in rat mesothelial cell cultures cytoplasmic lipid was only detected in a small subset of AM-cultured human mesothelial cells (data not shown). Control mesothelial cells cultured in normal growth medium did not show lipid accumulation at any time-point examined (data not shown).

Adipocytes are characterized by the expression of a number of protein markers which include; adipocyte fatty acid binding protein 4 (FABP4), lipoprotein lipase (LPL), CCAAT/enhancer binding protein α (CEBPα), adipocyte-specific peroxisome

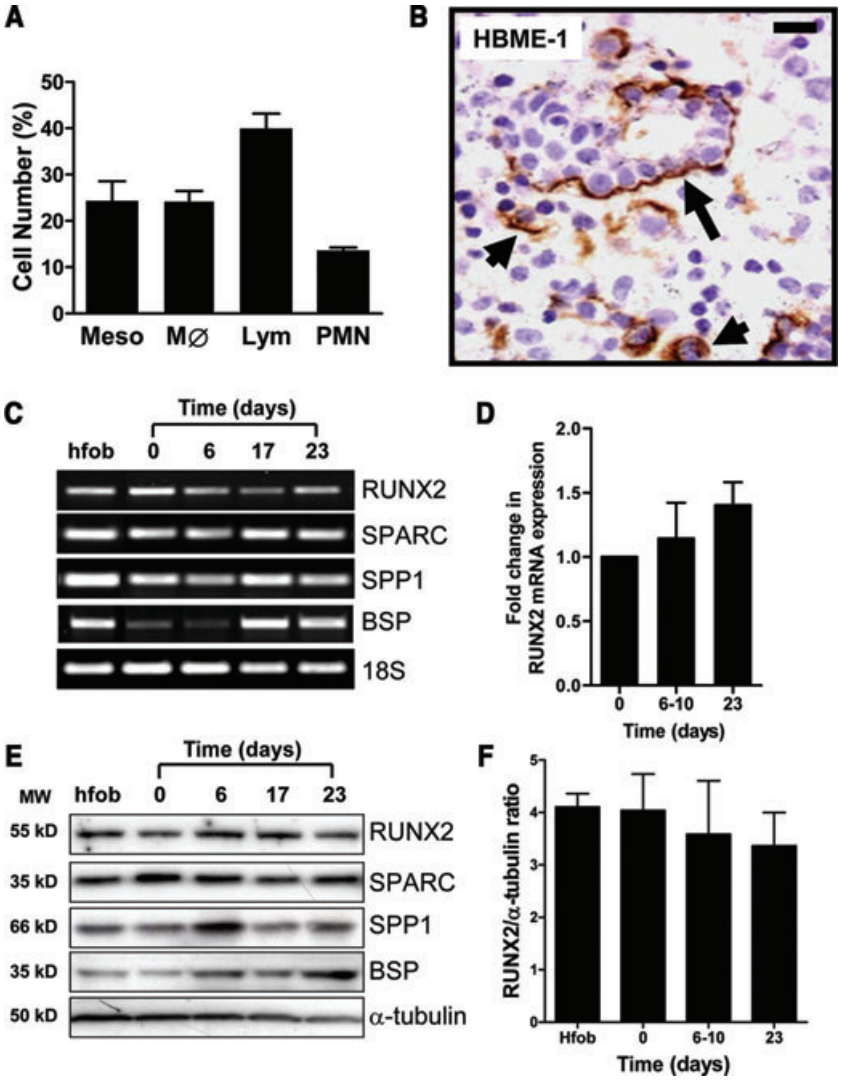

Fig. 7 Expression of osteoblast-associated genes and proteins in human mesothelial cells (**A**) Percentage of each cell type isolated from the pericardial fluid of four patients: mesothelial cells (Meso), macrophages (MØ), lymphocytes (Lym), polymorphonuclear neutrophils (PMN). (**B**) Human pericardial fluid cells immunostained for anti-HBME-1 demonstrating both individual (arrowhead) and sheets (arrow) of positively stained cells. Scale bar = 50 μm. (**C**) RT-PCR analysis of human mesothelial cells cultured in standard medium or OM for up to 23 days showing expression of osteoblast associated genes; RUNX2, SPARC, SPP1 and BSP). An hFOB was used as a positive control. (**D**) Quantification of Cbfa1 mRNA expression in three patients, expressed as fold change compared to day 0. (**E**) Western blot analysis of osteoblast phenotype markers. α-tubulin was used as a loading control. (**F**) Quantification of RUNX2 protein expressed in standard medium and OM stimulated human mesothelial cells up to 23 days in culture. Results shown are representative of three independent experiments.

proliferator-activated receptor γ2 (PPARγ2) and complement factor D (CFD) also called adipsin. Under resting conditions rat mesothelial cells expressed LPL and very low levels of CEBPα and FABP4 but required exposure to AM to induce expression of PPARγ and CFD (Fig. 8B). Unstimulated human mesothelial cells only expressed very low levels of FABP4 mRNA but expressed mRNA for all other markers following exposure to AM, which increased with time in culture (Fig. 8C).

Discussion

There are over 20 reported cases of MM with osseous and/or cartilaginous differentiation in the literature [13, 21] and bone and cartilage have been observed in MM induced by intraperitoneal injection of asbestos fibres in rats [22]. Several cases of mesenteric heterotopic ossification (or osseous metaplasia) [23, 24] and cartilaginous differentiation have also been reported in the peritoneum associated with sclerosing peritonitis [25, 26] and cartilage has been seen in peritoneal tissue biopsies not associated with malignancy or sclerosing peritonitis [27]. In the current study, foci of osseous metaplasia and mineralization were seen in human MM biopsy samples consistent with intratumoral bone formation. However, the frequency and extent of bone in these tumours could not be determined due to the small sample size of biopsy tissue. The mechanism for bone formation in these tumours is unknown although given the ability of mesothelial cells to differentiate into other cell types, including myofibroblasts, smooth muscle and endothelial cells, we suggest that adult

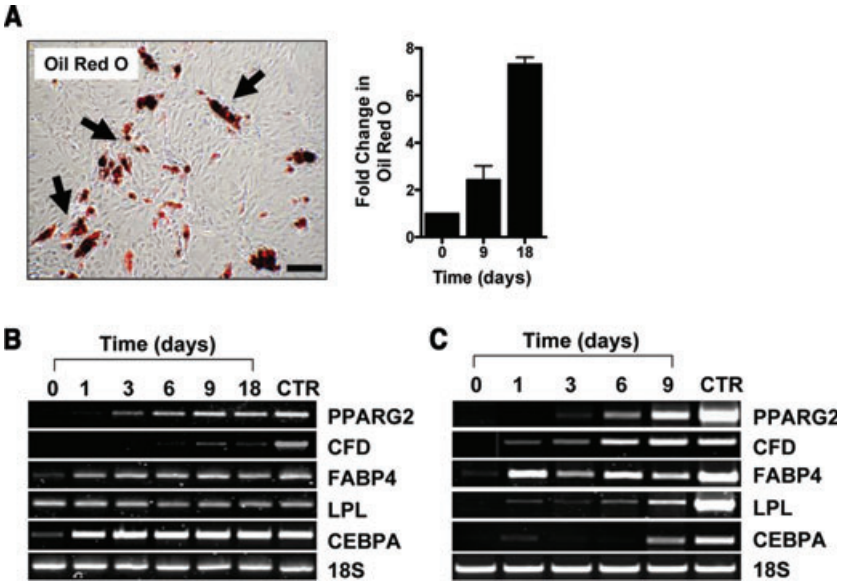

Fig. 8 Mesothelial cells accumulate lipid and express adipocyte markers. (**A**) Accumulated lipid, demonstrated by oil red O staining, was detected in rat mesothelial cell cultures exposed to AM for 18 days (black arrows). Scale bar = 100 μm. Quantitative analysis demonstrated a significant increase in lipid accumulation by these cultures over time, $***P < 0.001$. RT-PCR analysis of rat (**B**) and human (**C**) mesothelial cells cultured in standard medium or AM demonstrated the expression of mRNA associated with adipogenesis (PPARγ_2, CFD, LPL, CEBPα). cDNA derived from rat adipocytes and cells isolated from human subcutaneous fat were used as a positive control for the mature adipocyte phenotype (CTR). Results shown are representative of three independent experiments.

mesothelial cells retain the potential to differentiate into other cell types of embryonic mesoderm origin including an osteogenic and adipogenic lineage. To test this hypothesis, mesothelial cells were cultured in supplemented medium used to drive osteoblast and adipocyte differentiation and stages of differentiation compared with control BMMC-derived cells.

Characterization studies confirmed pure mesothelial cell cultures; however, rat cells were also FACS sorted using HBME-1 to conclusively eliminate any possible contaminating cells. Interestingly, only 30% of the total cell population were labelled with HBME-1 indicating down-regulation of this marker in culture. This was confirmed following culture of HBME-1$^+$ cells and subsequent restaining, with only 17% of cells immunopositive for HBME-1. Based on these findings and other characterization studies, it is likely that the original HBME-1$^-$ cells were also mesothelial cells. HBME-1$^+$ cells were also examined for a selection of stem cell markers. A proportion of cells were positive for CD90, CD73, CD146 and CD49e but negative for CD45, c-kit and STRO-1. The fact that the positively labelled cells also expressed HBME-1 suggests that a proportion of mesothelial cells may have mesenchymal stem cell-like properties although this needs further investigation.

Expression of a panel of proteins is also used to demonstrate differentiation of BMMC and other stem cell populations into osteoblasts *in vitro* [28, 29]. Total and HBME-1$^+$ sorted mesothelial cells expressed mRNA and protein for all markers similar to BMMC under the same conditions. The transcription factor RUNX2 is the only marker specific for the osteoblast lineage [30], however several isoforms have been identified in the human, mouse and rat with differing patterns of expression [31]. It is only the Cbfa1/OSF2 isoform of RUNX2 which is truly osteoblast specific [32] – referred to throughout this paper as RUNX2. Primers to identify this isoform were designed, as published primer sequences are not appropriate for the osteoblast-specific isoform. mRNA expression of RUNX2 increased over time in mesothelial cells cultured in OM although changes in protein were not demonstrated probably because the RUNX2 antibody was not specific for the bone-specific isoform.

Mesenchymal stem cells are derived from the embryonic mesoderm and retain expression of RUNX2 prior to differentiation to the osteoblast lineage yet still remain capable of entering multiple differentiation pathways [33]. mRNA expression of osteoblast-specific RUNX2 was also observed in untreated mesothelial cells, suggesting that these cells also retain the embryological potential of the mesoderm. Therefore, under the right conditions mesothelial cells differentiate into osteoblast-like cells and possibly other mesenchymal cell lineages in spite of being considered as terminally differentiated.

Transdifferentation is a reversible process involving the disruption of intercellular junctions and loss of apical-basolateral polarity, typically associated with epithelial cells, giving rise to fibroblast-like cells with pseudopodial protrusions and an increased migratory phenotype [34]. Transdifferentiation is measured by down-regulation of EMT markers such as cytokeratins and E-cadherin and increases in N-cadherin, αSMA, s100A4, MMP28 and SNAI1 [35–38]. Rat mesothelial cells cultured in OM demonstrated an EMT response, with CK19 expression down-regulated at day 26 while E-cadherin expression disappeared at day 6 but reappeared by day 18. Osteoblasts express high levels of E-cadherin [39], which is likely to explain the increase in E-cadherin by day 18. N-cadherin expression did not change but N-cadherin is normally expressed in mesothelial cells [40]. SNAI1 mRNA increased by day 5 which coincided with the decrease in E-cadherin, consistent with EMT. Although it is likely that mesothelial cells undergo transdifferentiation, we did not examine reversibility in this study and therefore we have used the term differentiation

instead of transdifferentiation following changes in mesothelial cell phenotype.

For a cell to be considered multipotent and to have adult stem cell-like potential, it must demonstrate differentiation into multiple mesenchymal cell lineages and express functional characteristics of the new cell types [41]. Therefore, the ability of mesothelial cells to differentiate into adipocyte-like cells was also examined. Acquisition of the mature adipocyte phenotype includes morphological cell rounding [42, 43], the accumulation of lipid-laden droplets in the cytoplasm and the induction of expression of adipocyte-specific genes [43]. Rat and human mesothelial cells cultured in AM demonstrated most of these features although consistent with osteoblast differentiation, there were differences in the ability of these cells to differentiate into a mature adipocyte phenotype. Oil red O staining clearly showed that many of the rat mesothelial cells cultured in AM contained lipid whereas very few human cells showed evidence of lipid accumulation. This may have been due to the human cells taking longer to differentiate as the human cells cultured in AM took longer to express mRNA for most of the adipocyte phenotype markers. The differential capacity for adipogenesis observed between rat and human cells may also be due to the frequency of adipogenic progenitors in each population, the optimum culture conditions required or the different origin of these cells. Although it is generally assumed that all mesothelium is similar irrespective of site or species, this still needs further investigation.

Conclusion

In conclusion, we have strong evidence that mesothelial cells retain the potential to differentiate along the embryonic developmental lines of the mesoderm, specifically into osteoblasts and adipocytes. This illustrates the multipotential nature of these cells and provides a mechanism by which bone is formed in MM tumours. Mesothelial cells have already been utilized in various tissue engineering applications, including the development of vascular conduits and peripheral nerve replacements [2]. The ability of mesothelial cells to differentiate along embryonic developmental lines suggests a far greater potential for these cells to be used for tissue engineering and regenerative medicine to repair, replace and possibly regenerate damaged or defective tissue at different sites in the body.

Acknowledgements

We thank Mr. Pierre Filion (PathWest Laboratory Medicine WA) for help with the TEM, Dr. Kathy Heel, Centre for Microscopy, Characterization and Analysis, University of Western Australia, for assistance with cell sorting and Dr. Stuart Hodgetts, University of Western Australia for provision of the CD90 antibody. This work was supported by grants from the Heart Foundation and National Health and Medical Research Council (grant no. 353554) of Australia and S.M.L. was supported by an Australian Commonwealth Postgraduate Award (and Lung Institute of Western Australia top up award).

Conflict of interest

The authors confirm that there are no conflicts of interest

Supporting Information

Additional Supporting Information may be found in the online version of this article:

Table S1 Primer sequences used for RT-PCR

Please note: Wiley-Blackwell is not responsible for the content or functionality of any supporting materials supplied by the authors. Any queries (other than missing material) should be directed to the corresponding author for the article.

References

1. **Mutsaers SE.** Mesothelial cells: their structure, function and role in serosal repair. *Respirology.* 2002; 7: 171–91.
2. **Herrick SE, Mutsaers SE.** Mesothelial progenitor cells and their potential in tissue engineering. *Int J Biochem Cell Biol.* 2004; 36: 621–42.
3. **Munoz-Chapuli R, Perez-Pomares JM, Macias D, *et al.*** Differentiation of hemangioblasts from embryonic mesothelial cells? A model on the origin of the vertebrate cardiovascular system. *Differentiation.* 1999; 64: 133–41.
4. **Perez-Pomares JM, Carmona R, Gonzalez-Iriarte M, *et al.*** Origin of coronary endothelial cells from epicardial mesothelium in avian embryos. *Int J Dev Biol.* 2002; 46: 1005–13.
5. **Perez-Pomares JM, Carmona R, Gonzalez-Iriarte M, *et al.*** Contribution of mesothelium-derived cells to liver sinusoids in avian embryos. *Dev Dyn.* 2004; 229: 465–74.
6. **Yang AH, Chen JY, Lin JK.** Myofibroblastic conversion of mesothelial cells. *Kidney Int.* 2003; 63: 1530–9.
7. **Kawaguchi M, Bader DM, Wilm B.** Serosal mesothelium retains vasculogenic potential. *Dev Dyn.* 2007; 236: 2973–9.
8. **Wada AM, Smith TK, Osler ME, *et al.*** Epicardial/Mesothelial cell line retains vasculogenic potential of embryonic epicardium. *Circ Res.* 2003; 92: 525–31.

9. **Decologne N, Kolb M, Margetts PJ, *et al.*** TGF-beta1 induces progressive pleural scarring and subpleural fibrosis. *J Immunol.* 2007; 179: 6043–51.
10. **Margetts PJ, Bonniaud P, Liu L, *et al.*** Transient overexpression of TGF-{beta}1 induces epithelial mesenchymal transition in the rodent peritoneum. *J Am Soc Nephrol.* 2005; 16: 425–36.
11. **Yanez-Mo M, Lara-Pezzi E, Selgas R, *et al.*** Peritoneal dialysis and epithelial-to-mesenchymal transition of mesothelial cells. *N Engl J Med.* 2003; 348: 403–13.
12. **Kiyozuka Y, Miyazaki H, Yoshizawa K, *et al.*** An autopsy case of malignant mesothelioma with osseous and cartilaginous differentiation: bone morphogenetic protein-2 in mesothelial cells and its tumour. *Dig Dis Sci.* 1999; 44: 1626–31.
13. **Klebe S, Mahar A, Henderson DW, *et al.*** Malignant mesothelioma with heterologous elements: clinicopathological correlation of 27 cases and literature review. *Mod Pathol.* 2008; 21: 1084–94.
14. **Yousem SA, Hochholzer L.** Malignant mesotheliomas with osseous and cartilaginous differentiation. *Arch Pathol Lab Med.* 1987; 111: 62–6.
15. **Donna A, Betta PG.** Mesodermomas: a new embryological approach to primary tumours of coelomic surfaces. *Histopathology.* 1981; 5: 31–44.
16. **Bellows CG, Aubin JE, Heersche JN, *et al.*** Mineralized bone nodules formed *in vitro* from enzymatically released rat calvaria cell populations. *Calcif Tissue Int.* 1986; 38: 143–54.
17. **Foley-Comer AJ, Herrick SE, Al-Mishlab T, *et al.*** Evidence for incorporation of free-floating mesothelial cells as a mechanism of serosal healing. *J Cell Sci.* 2002; 115: 1383–9.
18. **Katoh J, Ishida Y, Taniguchi H.** Isolation of preadipocytes from rat adipose tissue *in vitro*. *Folia Histochem Cytobiol.* 1994; 32: 235–8.
19. **Sherwood AL, Mutsaers SE, Peeva VK, *et al.*** Spontaneously immortalized mouse mesothelial cells display characteristics of malignant transformation. *Cell Prolif.* 2008; 41: 894–908.
20. **Ramirez-Zacarias JL, Castro-Munozledo F, Kuri-Harcuch W.** Quantitation of adipose conversion and triglycerides by staining intracytoplasmic lipids with Oil red O. *Histochemistry.* 1992; 97: 493–7.
21. **Demirag F, Unsal E, Tastepe I.** Biphasic malignant mesothelioma cases with osseous differentiation and long survival: a review of the literature. *Lung Cancer.* 2007; 57: 233–6.
22. **Rittinghausen S, Ernst H, Muhle H, *et al.*** Atypical malignant mesotheliomas with osseous and cartilaginous differentiation after intraperitoneal injection of various types of mineral fibres in rats. *Exp Toxicol Pathol.* 1992; 44: 55–8.
23. **Hansen O, Sim F, Marton PF, *et al.*** Heterotopic ossification of the intestinal mesentery. Report of a case following intraabdominal surgery. *Pathol Res Pract.* 1983; 176: 125–30.
24. **Yannopoulos K, Katz S, Flesher L, *et al.*** Mesenteritis ossificans. *Am J Gastroenterol.* 1992; 87: 230–3.
25. **Nakazato Y, Yamaji Y, Oshima N, *et al.*** Calcification and osteopontin localization in the peritoneum of patients on long-term continuous ambulatory peritoneal dialysis therapy. *Nephrol Dial Transplant.* 2002; 17: 1293–303.
26. **Rigby RJ, Hawley CM.** Sclerosing peritonitis: the experience in Australia. *Nephrol Dial Transplant.* 1998; 13: 154–9.
27. **Fadare O, Bifulco C, Carter D, *et al.*** Cartilaginous differentiation in peritoneal tissues: a report of two cases and a review of the literature. *Mod Pathol.* 2002; 15: 777–80.
28. **Aubin JE.** Advances in the osteoblast lineage. *Biochem Cell Biol.* 1998; 76: 899–910.
29. **Aubin JE.** Bone stem cells. *J Cell Biochem Suppl.* 1998; 72: 73–82.
30. **Harada H, Tagashira S, Fujiwara M, *et al.*** Cbfa1 isoforms exert functional differences in osteoblast differentiation. *J Biol Chem.* 1999; 274: 6972–8.
31. **Xiao ZS, Thomas R, Hinson TK, *et al.*** Genomic structure and isoform expression of the mouse, rat and human Cbfa1/Osf2 transcription factor. *Gene.* 1998; 214: 187–97.
32. **Ducy P, Zhang R, Geoffroy V, *et al.*** Osf2/Cbfa1: a transcriptional activator of osteoblast differentiation. *Cell.* 1997; 89: 747–54.
33. **Stewart K, Walsh S, Screen J, *et al.*** Further characterization of cells expressing STRO-1 in cultures of adult human bone marrow stromal cells. *J Bone Miner Res.* 1999; 14: 1345–56.
34. **Hay ED.** An overview of epithelio-mesenchymal transformation. *Acta Anat.* 1995; 154: 8–20.
35. **Maeda M, Johnson KR, Wheelcock MJ.** Cadherin switching: essential for behavioural but not morphological changes during an epithelium-to-mesenchyme transition. *J Cell Sci.* 2005; 118: 873–87.
36. **Nasreen N, Mohammed KA, Mubarak KK, *et al.*** Pleural mesothelial cell transformation into myofibroblasts and haptotactic migration in response to TGF-beta1 *in vitro*. *Am J Physiol Lung Cell Mol Physiol.* 2009; 297: L115–24.
37. **Rodgers UR, Kevorkian L, Surridge AK, *et al.*** Expression and function of matrix metalloproteinase (MMP)-28. *Matrix Biol.* 2009; 28: 263–72.
38. **Tanjore H, Xu XC, Polosukhin VV, *et al.*** Contribution of epithelial-derived fibroblasts to bleomycin-induced lung fibrosis. *Am J Respir Crit Care Med.* 2009; 180: 657–65.
39. **Cheng SL, Lecanda F, Davidson MK, *et al.*** Human osteoblasts express a repertoire of cadherins, which are critical for BMP-2-induced osteogenic differentiation. *J Bone Miner Res.* 1998; 13: 633–44.
40. **Simsir A, Fetsch P, Mehta D, *et al.*** E-cadherin, N-cadherin, and calretinin in pleural effusions: the good, the bad, the worthless. *Diagn Cytopathol.* 1999; 20: 125–30.
41. **Dominici M, Le Blanc K, Mueller I, *et al.*** Minimal criteria for defining multipotent mesenchymal stromal cells. The International Society for Cellular Therapy position statement. *Cytotherapy.* 2006; 8: 315–7.
42. **Gregoire FM, Smas CM, Sul HS.** Understanding adipocyte differentiation. *Physiol Rev.* 1998; 78: 783–809.
43. **Rosen ED, Walkey CJ, Puigserver P, *et al.*** Transcriptional regulation of adipogenesis. *Genes Dev.* 2000; 14: 1293–307.